Understanding the acoustics of Papal basilicas in Rome by means of a coupled-volumes approach

Postprint version of the paper published in the Journal of Sound and Vibration 382(2016), 413-427. **DOI: 10.1016/j.jsv.2016.07.007**

Understanding the acoustics of Papal basilicas in Rome by means of a coupled-volumes approach

Francesco Martellotta

Dipartimento di Scienze dell'Ingegneria Civile e dell'Architettura, Politecnico di Bari, via Orabona 4, I-70125 Bari, Italy. email address: francesco.martellotta@poliba.it

Abstract

The paper investigates the acoustics of the World-famous four Papal Basilicas in Rome, namely Saint Peter, St. John Lateran, St. Paul outside the Walls, and Saint Mary Major. They are characterized by different dimensions, materials, and architectural features, as well as by a certain number of similarities. In addition, their complexity determines significant variation in the acoustics depending on the relative position of source and receivers. A detailed set of acoustic measures was carried out in each church, using both spatial (B-format) and binaural microphones, and determining the standard ISO 3382 descriptors. Results are analyzed in relation to the architectural features, pointing out the differences observed in terms of listening experience. Finally, in order to explain some of the results found among energy-based parameters, churches were analyzed as a system of acoustically coupled volumes. The latter explained most of the anomalies observed in the distribution of acoustic parameters, while showing at the same time that secondary spaces (aisles, chapels) play a different role depending on the amount of sound absorption located into the main nave.

Keywords: Church acoustics, coupled volumes, analytical acoustic model, acoustic environment, listening experience

This is a postprint version. Please cite this paper as: Martellotta F., "Understanding the acoustics of Papal basilicas in Rome by means of a coupled-volumes approach", Journal of Sound and Vibration 382(2016), 413-427. DOI: 10.1016/j.jsv.2016.07.007

Postprint version of the paper published in the Journal of Sound and Vibration,
DOI: 10.1016/j.jsv.2016.07.007

1. Introduction

Church acoustics gained significant attention in the last 20 years, resulting in a variety of contributions from different countries [1-14] and involving different aspects such as the way sound propagates inside them [8,15,16], the role of occupancy [6,18,19], the relationship with liturgy and music [21,21], the definition of rating schemes for optimal listening conditions [22,23], the use of innovative technologies to virtually reproduce buildings that have been destroyed or modified [24,25]. The need to correctly design the acoustics of new churches, and adapt the old ones, prompted books on this topic [26,27]. However, despite the large amount of published research, the complexity and uniqueness of each building, resulting from the historical stratification of architectural styles, and addition/replacement of different elements or entire volumes, makes any generalization difficult to be applied. Consequently, any acoustic investigation of individual buildings may offer occasions to better understand some of the uniqueness features and the related fundamental problems.

The present study aims at characterizing the acoustics of the four Papal Basilicas in Rome (formerly known as Patriarchal Basilicas), namely Saint Peter (SPB), St. John Lateran (SJL), St. Paul outside the Walls (SPX), and Saint Mary Major (SMM). All of them have been investigated in the past and are the subject of two of the earliest researches in the field of church acoustics. In fact in 1953 Raes and Sacerdote [28] analyzed SJL and SPX, while twenty years later Shankland and Shankland [29] measured reverberation time in SPB and in the other three Papal Basilicas by means of a tape recorder and by ear and stopwatch. Despite the very rudimentary equipment, some of the key features of these spaces were identified. The most surprising being the mid-frequency reverberation time of 7.1 s measured in SPB, a value lower than those observed in other much smaller churches[5]. Double slope decays were observed in SJL when the source was moved inside the aisle. The origin of the unusual behavior observed in SPB was analyzed and explained recently[17], taking advantage of more sophisticated measurement techniques and interpreting the results within the framework of coupled-volume systems. Use of Bayesian analysis [30] and the representation of the space as a system of acoustically coupled volumes [31], successfully tested in St. Paul Cathedral in London [32], contributed to explain that reduced reverberation time mostly depended on increased absorption due to richly decorated surfaces. In the present paper, the same techniques were applied to the whole set of the Papal Basilicas, first describing their acoustical properties in terms of reverberation and other acoustical parameters, and then explaining the observed behavior as a function of the architectural features of the spaces, with particular reference to the effect of coupled volumes.

2. Methods

2.1. Measurement techniques

Measurements were carried out complying with ISO 3382-1 standard[33], together with a set of guidelines specifically defined for churches[7]. The measurements were carried out using omni-directional sound sources (a Look-Line D301 and a self-made dodecahedron made of twelve 120 mm loudspeakers), each one combined with an additional sub-woofer to cover low frequencies. Each sound source was fed by a different constant-envelope equalized sine sweep (40 s long) generated using MATLAB according to Müller and Massarani[34] so that the spectrum of the radiated sound was substantially flat from the 50 Hz to the 16 kHz third-octave bands. Impulse responses (IRs) were collected by using a B-format microphone (Soundifield Mk-V) and a binaural head and torso (B&K 4100D) connected to an Echo Audio Layla 24 sound card. In SPB additional microphones were used to speed up the measurements and they included a Neumann TLM-127 with variable polar pattern, allowing the measurement of both omni-directional and figure-of-eight IRs, and an omni-directional microphone (GRAS 40-AR) connected to a portable recorder to get IRs in the farthest positions. In all the cases the room responses were recorded at a sampling rate of 48 kHz and 24 bit depth, to obtain, after deconvolution (performed using MATLAB), IRs with a signal-to-noise ratio which allowed a "safe" calculation of reverberation time (T_{30}) based on at least 30 dB of decay.

In each church several source-receiver combinations were analyzed, with a minimum of two sources and 13 to 32 receivers usually placed in one half of the church (Figure 1). The source and the microphones were 1.5 m and 1.2 m from the floor surface, respectively. The B-format microphone pointed with the X axis toward the sound source, while the binaural head was placed on the seat facing the altar (with no head rotation). The whole set of IRs collected in this way was later used to calculate the most important acoustical parameters according to the ISO 3382-1 standard [33].

2.2. Surveyed churches

The building of the Basilica of Saint Mary Major (Fig 2a) started in 432, following a simple three naves basilica scheme. Several modifications were added later. The Cosmatesque floor dates 12th century, while the transept was added at the end of the 13th century. Each brace of the transept terminates in a chapel (both realized in later times) having the dimensions of small church and being directly connected to the main volume of the basilica. During the 15th century the central nave was covered by the richly decorated and deeply coffered ceiling, finished by gold leafs. The aisles are vaulted and finished in plaster. The total length is about 80 m, and the width at the transept is 35 m. The nave width is 17 m and the height is 18.6 m. The resulting overall volume (chapels excluded) is 38000 m^3.

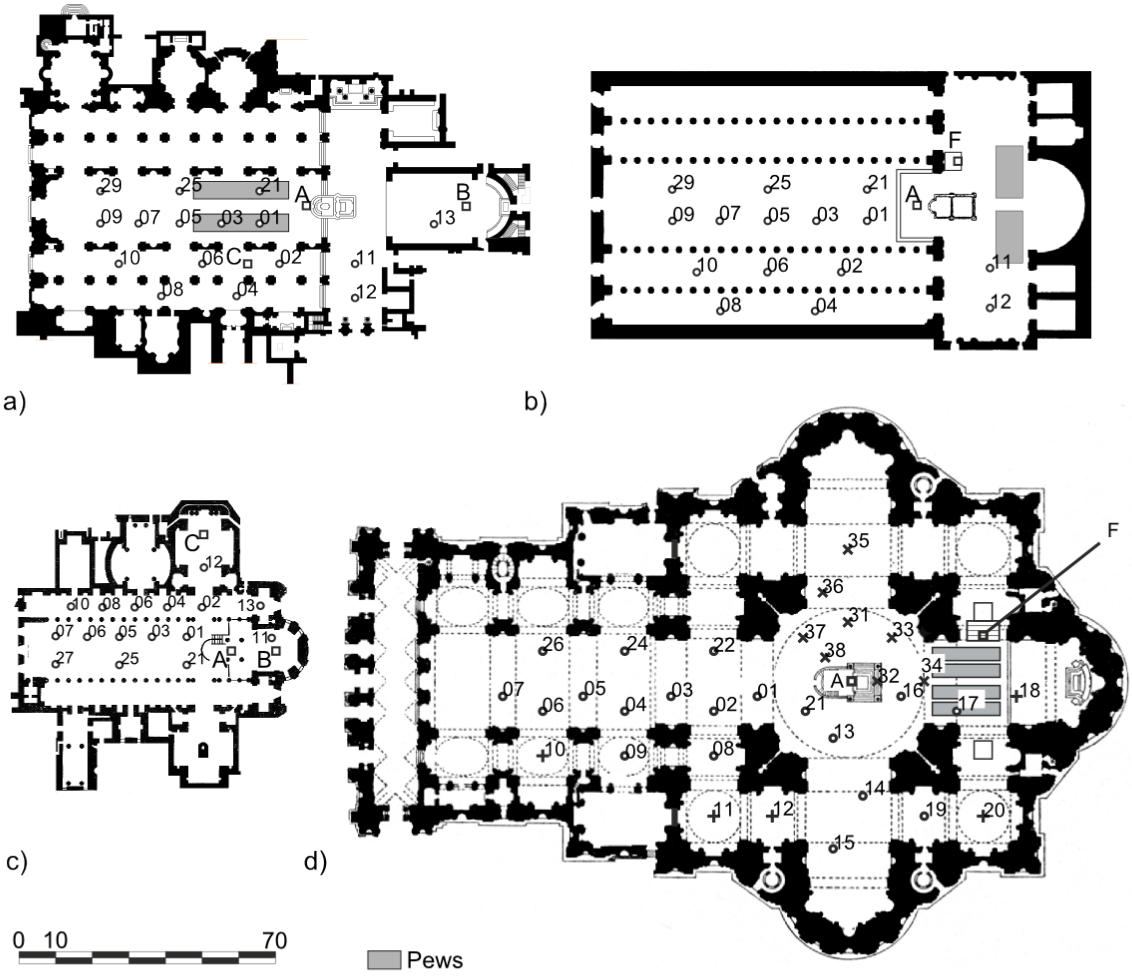

Figure 1 – Plan of the four basilicas with indication of the source and receiver positions. Capital letters correspond to sources, numbers to receivers. a) SJL; b) SPX; c) SMM; d) SPB

The Basilica of St. John Lateran (Fig 2b) was consecrated in 324 and is consequently the oldest of the Major Roman Basilicas. However, its present appearance is mostly due to the restoration works that were carried out around 1650 and directed by Francesco Borromini. The columns that divided the central nave from the aisles were grouped to form massive piers, thus creating a marked division between the volumes. The columns subdividing the aisles were also thickened and a new decorative pattern was applied over all surfaces. The existing richly coffered ceiling and the Cosmatesque marble floor were not touched at this stage. At the end of 19th century the apse was reconstructed and enlarged to include a wooden choir. The total length is 130 m, and the width at the transept is 69 m. The nave width is 18 m, and the height is 25 m. The overall volume is consequently about 120000 m^3.

Postprint version of the paper published in the Journal of Sound and Vibration,
DOI: 10.1016/j.jsv.2016.07.007

Figure 2 – Interior view of the four surveyed churches. a) SMM; b) SJL; c) SPX; d) SPB.

The Basilica of Saint Paul outside Walls (Fig 2c) was founded by Emperor Constantine I in the 4th century and almost immediately expanded to become the largest church in Rome (and it remained so until St. Peter was rebuilt). Despite many additions the church maintained its original Early-Christian character until 1823, when a fire destroyed it almost completely. The church was rebuilt and reconsecrated in 1855 maintaining the original structure. The church is 131 m long, 65 m wide, and about 30 m high. The overall volume is consequently about 160000 m^3.

The building of St. Peter's Basilica (Fig 2d) started in 1506, and was finally consecrated in 1626, even though decorative works went on for several years. Its huge dimensions are characterized by a total length of 185 m, a nave width of about 26 m, and a dome width of 41.5 m and height (up to the lantern) of about 120 m. The resulting volume of the basilica is about 500000 m^3. Most of the surfaces are finished in plaster, marble or stucco, but they are richly decorated with deep carvings. Pews (with upholstered kneelers) are permanently installed in the choir, while the remaining floor areas are normally bare. At the center of the main nave a wooden barrier is installed to protect the central part of the floor. A summary of the key features of the four churches is given in Table 1.

Table 1
Summary of the geometrical and acoustic details of surveyed churches

	ID	*V* *[m³]*	*S* *[m²]*	S_{floor} *[m²]*	*Temp.* *[°C]*	*RH* *[%]*	$T_{30(500\text{-}1k)}$ *[s]*
Saint Peter's Basilica	SPB	500,000	80,000	12,600	21	60%	9.91
Basilica of Saint Paul outside Walls	SPX	160,000	33,000	8,000	21	75%	8.25
Basilica of St. John Lateran	SJL	120,000	26,000	5,800	21	70%	5.86
Basilica of Saint Mary Major	SMM	38,000	12,000	2,700	23	62%	4.30

3. Experimental results

3.1. Reverberation time

The four churches had significantly different dimensions, so reverberation time (T_{30}) was expected to vary a lot among them. As shown in Fig. 3, the longest and the shortest T_{30} were observed, respectively in the largest (SPB) and smallest (SMM) of the four churches. In SPB the longest values were observed at 125 Hz, with an average value of 13.6 s, decreasing to 2.0 s at 8 kHz. In SMM the longest values were found below 500 Hz where T_{30} was about 4.7 s on average, decreasing to 1.7 s at 8 kHz. For the two intermediate churches the differences in T_{30} were larger than it could be expected by considering their room volumes. In fact, in SPX the longest T_{30} was 9.3 s at 250 Hz, decreasing to 2.3 at 8 kHz, while in SJL the longest T_{30} was 6.4 s at 125 Hz, decreasing to 2 s at 8 kHz.

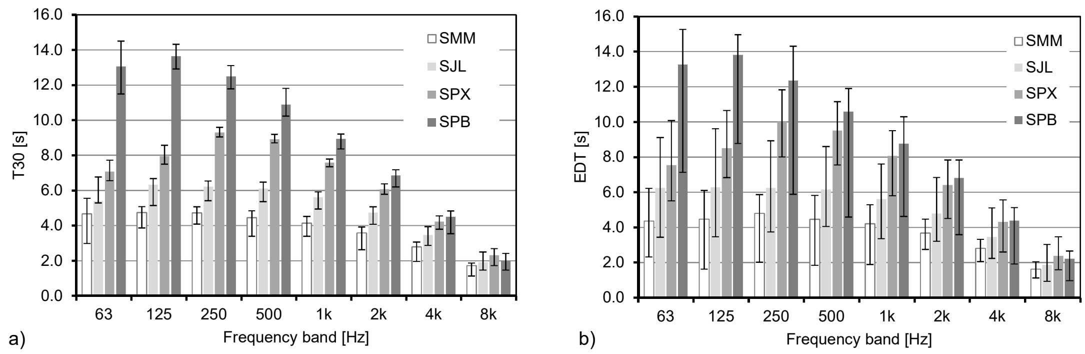

Figure 3 – a) Reverberation time (T_{30}) and b) Early decay time as a function of frequency for the four basilicas. Error bars represent maximum and minimum values observed in each church

As in all large rooms, the role of air absorption at high frequencies was particularly significant. The substantially identical T_{30} value observed at 8 kHz resulted from air absorption being the largest contributor to sound absorption, so that, in agreement with classical formulas, the T_{30} value was independent of room volume. Conversely, at low frequencies the situation was more varied. As in SMM and in SJL the trend as a

DOI: 10.1016/j.jsv.2016.07.007

function of frequency was rather flat at low frequencies, a feature generally found in churches with a mixed presence of wooden surfaces (usually richly decorated), and equally decorated plaster surfaces. A similar behavior was found also in SPB, even though the room dimensions and the lack of a wooden ceiling clearly explained the much longer values. On the other hand, in SPX the presence of the peak at 250 Hz, and the regular decrease appearing at 125 and 63 Hz denoted the presence of surfaces markedly absorbing low frequencies (likely the wooden ceiling covering the side aisles).

The analysis of the T_{30} variations inside each church showed that SPX was the church with the most uniform T_{30} distribution. Slightly larger variations appeared in the other churches (particularly at low frequencies), but, as it will be clarified by the analysis of the other acoustic parameters, the anomalies were mostly due to less reverberant sub-volumes (like choirs).

The analysis of EDT showed that, on average, the values as a function of frequency were similar to T_{30} (Fig. 3b). However, as expected, the variations within each church were much larger, independent of the church considered. EDT is known to be very sensitive to early reflection distribution and, particularly in large churches, it follows a typical trend in which it assumes short values at receivers close to the source (where direct sound and early reflections are strong), and gradually grows as the distance increases as a consequence of the lack (or the weakening) of early reflections [16]. Such behavior is typical of systems of weakly coupled volumes (as it was demonstrated for SPB [17]), but in churches it regularly appears in single volumes (such as the central nave), so that treating them as the addition of adjacent sub-spaces proved successful [8]. As a consequence, a dependence of EDT as a function of distance appears and from its analysis several elements of discussion can arise. Figure 4 shows such plot for the churches under analysis. Churches were grouped to ease the analysis as they showed clearly different behaviors. In fact, the rate of variation for SMM and SPX, which both share the presence of thin columns dividing the naves, was about 2 s/100 m, substantially smaller than for the other two churches. In SMM only a few points showed oddly long EDT and they corresponded to source receiver combinations in which either the source or the receiver (but not both) were in the chapel. Conversely, combination B-11 showed a markedly shorter EDT which required further analysis to understand whether this depended on different acoustic characteristics of the sub-volume compared to the rest of the church. In SPX the trend was very similar for both source positions, but source F had EDT values 1 to 2 s longer. In this case the position of the source close to the organ prevented nearly all the receivers from getting direct sound and relevant early reflections. Thus the decay curve systematically showed horizontal tangent at t=0, with consequently longer EDT values.

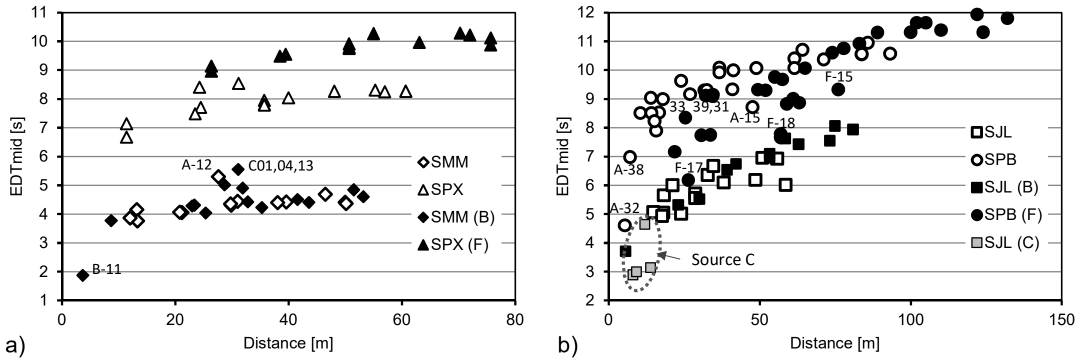

Figure 4 – Plot of EDT values at mid frequencies (500-1000 Hz) as a function of source receiver distance and source position. a) SMM and SPX; b) SJL and SPB.

For the SJL and SPB pair (Fig. 4b) the rate of variation was higher. In particular, in SPB the rate was higher when source was in the choir (4.8 s/100 m) than when it was in the crossing (2.7 s/100m). Explanation for this behavior was found [17] to be related to the choir being weakly coupled to the main nave. Several outliers appeared also in this case, showing shorter (F-15, F-18, A-15), or longer (F-31,F-33,F-39) values compared to distance. Different amounts of initial energy, largely depending on the large pillars supporting the dome, explained the differences

Finally, in SJL different rates of variations were observed depending on source positions, with a slope of 3.5 s/100 m for the source in the nave, and 5.4 s/100 m for the source in the choir. The shortest EDT values, varying between 3 and 4 s, were observed when both source and receivers were either in the choir (B-13) or in the aisles (C-02,04), suggesting once again that weak acoustic coupling took place and that, despite the long reverberation time, more intimate acoustic conditions were experienced there.

As an evidence supporting the above observations, Bayesian analysis [30] was applied to a selection of source-receiver combinations belonging to the different churches. Results confirmed (Fig. 5) that choirs and aisles showed a two-slope decay when the source was in the same sub-space. In fact, the steeper initial decay appeared in all the cases as being sufficiently diffuse and lengthy to be considered a proper decay rather than just the effect of discrete early reflections. The same analysis applied to receivers located in the same sub-space of the source but characterized by larger volume (or much larger openings) showed nearly undetectable double decays. Likely, this depended on a large fraction of the emitted energy going directly into adjacent sub-volumes. In the light of above results a more detailed analysis on the effect of acoustical coupling was carried out in Sect. 4.2.

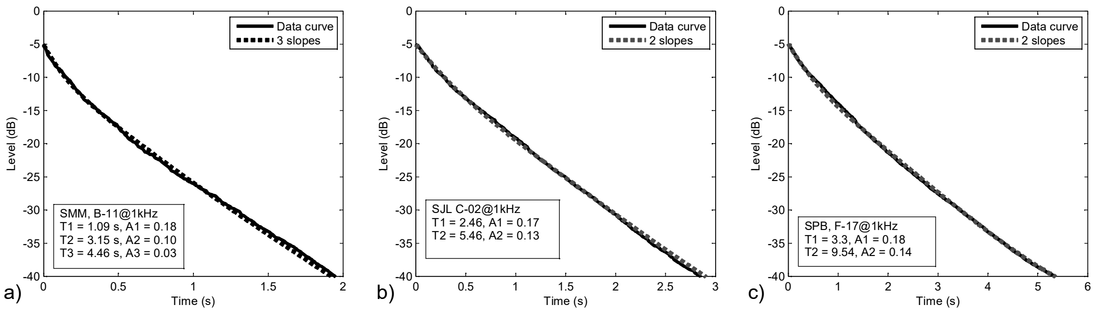

Figure 5 – Plot of double decays identified in different churches. a) SMM, combination B-11; b) SJL, combination C-02; c) SPB, combination F-17

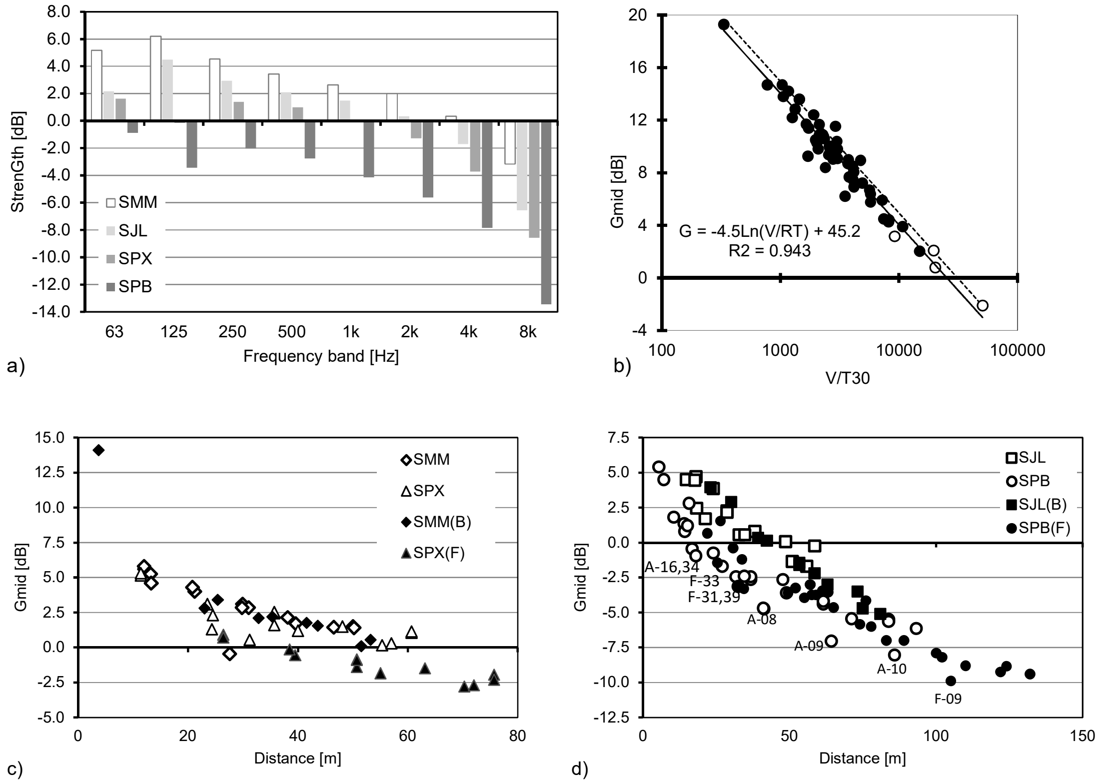

Figure 6 – Plot of strength values as a function of frequency (a), and mid frequency average as a function V/T30 ratio (b) and of source receiver distance (c,d).

3.2. Sound strength

According to diffuse field theory, sound strength (G) should decrease linearly with the logarithm of the volume to reverberation time ratio. Therefore, as the four basilicas are among the largest churches in the World and, as observed, their reverberation time was short (compared to volume), a relatively low value for G was expected. Figure 6a confirmed this, showing for all the churches a decrease as a function of frequency,

DOI: 10.1016/j.jsv.2016.07.007

coherently with the T_{30} reduction due to air absorption. Considering the overall average, only SMM and SJL had positive values at mid frequencies (respectively 3.0 dB and 1.8 dB). Despite the longer reverberation, both SPX and SPB had negative mid-frequency averages, respectively equal to –0.3 dB and –3.4 dB, as an obvious consequence of the larger (much larger for SPB) volume. A quick comparison with the average G values measured in a number of other churches [5] plotted as a function of V/T_{30} showed that the four basilicas were in very good agreement with the other measurements (Fig. 6b).

However, despite the good agreement between theoretical values and average measured values, G is known to have dependence as a function of source receiver distance. Figure 6c,d confirmed this dependence with some interesting similarities with the EDT plot. In fact, in SMM G values showed a mild decreasing trend as a function of distance, with no substantial anomaly except for combinations B-11 and A-12. In both cases a different energy distribution among sub-volumes may explain the result. In the first case, source and receiver were in the same sub-volume, while in the latter the value was about 3 dB lower than other points at the same distance. As the chapel is connected to the main volume through a single opening it is likely to have a lower energy density due to weak coupling. In SPX the G values corresponding to source F showed differences of about 2 dB compared to points at the same distance but fed from source A, confirming what was observed for EDT. In SJL the values were more uniformly distributed, particularly for source B. For source A slight variations appeared, generally not exceeding 2 dB, between receivers at the same distance from the source, but located in the aisles. In SPB a more scattered distribution appeared. In particular, when source was at the altar a 3 dB difference appeared between receivers in the main nave and those in the aisles (08, 09, 10), while similar differences appeared at receivers around the altar. Sometimes such differences could be attributed to lack of direct sound, while in other cases direct sound and early reflection had not enough energy to justify the difference, which was more likely attributed to different energy distribution among sub-volumes. With reference to source F, the trend as a function of distance was more regular at farthest points, while receivers close to the source were split into two sub-sets. As for EDT receivers showing the lowest G values compared to their actual distance were those located behind the large pillar supporting the dome.

3.3. Energy ratios

Among the different energy ratios only centre time (T_S) and clarity (C_{80}) were considered. In fact, T_S is certainly preferable as it does not depend on arbitrary choice of “useful” and “detrimental” time intervals. However, C_{80} despite being flawed by that arbitrary choice is now widely used and allows an immediate comparison with reference values. Figure 7 showed that both parameters followed a general trend that clearly reminded what was observed for EDT and G before. So, SMM was the church with the lowest T_S, even at the farthest receivers (and independent of the source position). In

SPX the usual difference between source A and B appeared (with an average difference of about 450 ms), but the increase as a function of distance was regular. For clarity the same considerations applied, but the difference between the two churches was considerably attenuated and the points in the scatterplot were superimposed (only for source A in SPX). Three factors contributed to explain such behaviour. First, the two churches had a different reverberant radius, being about 8 m in SPX and 5.4 m in SMM. Then, in SMM the nave floor was covered by seats, which prevented any strong reflection from the floor to get to the receivers. Finally, in SMM the source was located in front of the high altar but behind the opening to access the crypt, while in SPX the source was located in front of the opening to access the crypt, thus ensuring stronger floor reflections. It is worth pointing out that Ts was less sensitive to such subtle variations, being more strictly related to the length of the reverberant tail and to the energy distribution among sub-volumes.

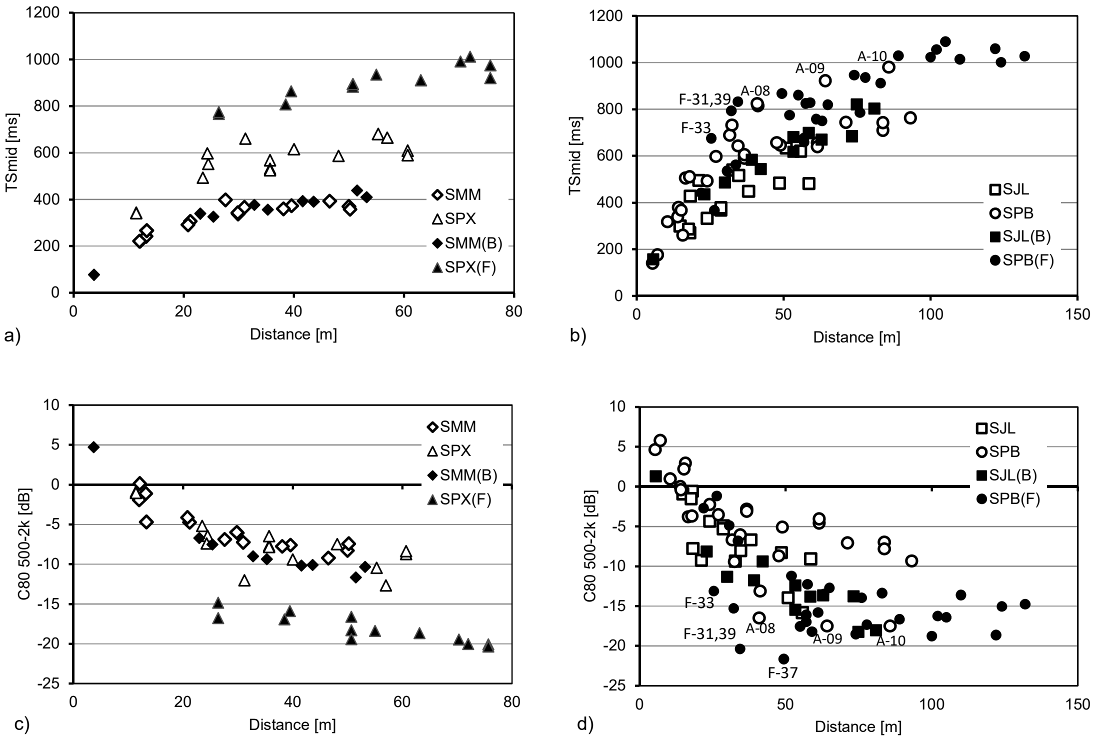

Figure 7 – Plot of multi-octave band average values of center time (a,b) and clarity (c,d) as a function of source receiver distance.

In SJL T_S values in the nave were about 200 ms shorter than those measured in the aisles when source was in A, while moving the source to B minimized the differences. Thus the effect of the large pillars dividing the nave from the aisles was certainly evident in this church, while in SMM or SPX the thinner columns were less obstructing, so energy density was more evenly distributed. Comparing only receivers in the nave, SJL had lower T_S values than SPX, in agreement with its lower T_{30} and stronger early reflections due to pillars.

SPB showed the largest variations and the most scattered behaviour. In most of the cases the same anomalies observed discussing the other parameters were found. So, receivers 08, 09, and 10 showed apparently odd behaviour when source was in A, while receivers 31, 33, 37, and 39 showed the largest discrepancy when source was in F. In both cases the lack of early energy was responsible for this result. However, the analysis of C_{80} values pertaining to source A showed the most surprising results. In fact, at equal distances the values measured in SPB were markedly higher than those observed in the other churches, despite the much longer reverberation. When source was moved to F, C_{80} values proved to be as low as those observed in SPX under the same conditions. Again, the reverberant radius in SPB was 12.8 m (as a consequence of the lower energy density caused by the huge volume). Thus the reverberant tail, although longer, brought a lower amount of "detrimental" energy. In addition, the analysis of measured IRs showed that in SPB an important contribution came from the large pillars that allowed strong reflections to get to the receiver within the first 80 ms. To confirm the above hypothesis, a comparison between decay curves at 1 kHz taken at distances between 36 and 39 m in different churches showed (Fig. 8) that in SPB the decay curve was concave, while in the other churches it was convex (with a nearly horizontal tangent at t=0). Thus in SPB direct sound was much stronger than late reverberant sound.

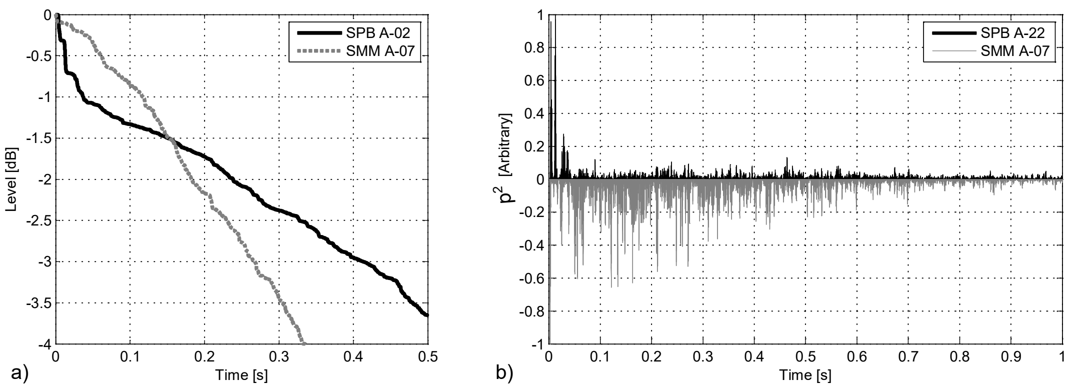

Figure 8 – a) Plot of early decay curves at receivers at approximately the same distance in SPB, SMM, and SJL. b) Plot of the squared pressure measured at the same receivers in SPB and SMM.

3.4. Spaciousness descriptors

Measured spaciousness descriptors included both the inter-aural cross correlation coefficient (1–IACC) and the lateral fraction (J_{LF}), both referred to the 80 ms interval. However, as they are known to be substantially correlated, for the sake of brevity only the first was considered by taking into account the average calculated over the octave bands from 500 to 2000 Hz. In this case plotting the values as a function of distance usually offers little advantage because of the significant scattering [35], consequently, a simpler statistical analysis of the occurrence of the different values was carried out for each church and for each source position.

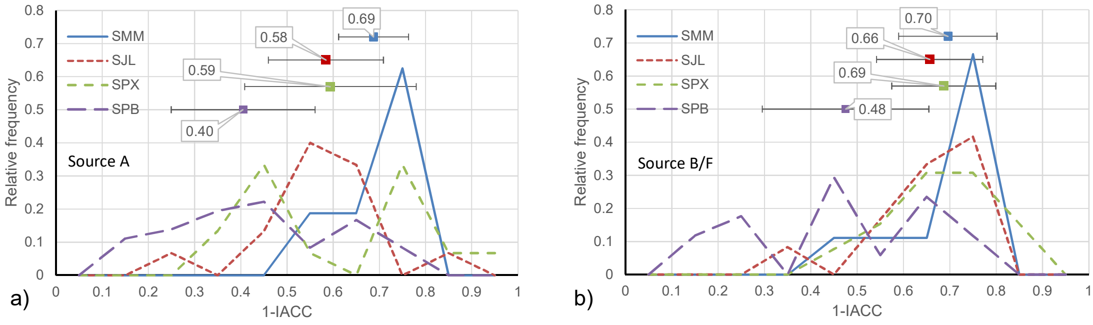

Figure 9 – Plot of frequency distribution (with mean and standard deviations represented by error-bars) of 1–IACC values inside different churches as a function of source position. a) Source A; b) Source B/F

Results showed (Fig. 9) that in SMM for source A most of the receivers had 1–IACC values varying between 0.6 and 0.8, with an average of 0.69. When source was moved in B a slight increase in the values was observed (average was 0.70), even though the low value observed in B-11 increased the standard deviation. In SJL the distribution was nearly normal for both source positions. However, placing the source in the choir caused an increase by 0.08 in 1–IACC due to generally higher values observed throughout the church as all receivers benefited from a less coherent signal. In SPX the distribution was almost bi-modal when source was in A. In fact, receivers in the nave, characterized by a mostly frontal sound, had values that, on average, were 0.23 smaller than those in the aisles (which benefited from sound diffracted by columns, which was intrinsically less coherent [36]). To confirm this, when the source was moved to F the difference disappeared and all the values were almost normally distributed around the mean value of 0.69. Finally, in SPB the lowest average values appeared together with a large standard deviation. Very low values were measured in the nave, where the average 1-IACC was 0.33 for source A, and 0.36 for source F. An increase was observed when receivers in the aisles, transept, and choir were considered, allowing the overall average to raise to 0.40 for source A and 0.48 for source F. In the first case most receivers were exposed to direct sound which, being much louder than reflections (due to low energy density) caused high correlation of binaural signals. Conversely when source was in F this effect was strongly reduced.

4. Discussion

4.1. Analysis of listening conditions

At the end of this analysis the listening conditions inside the surveyed churches could be discussed. As the measurements were carried out under unoccupied conditions any reference to "optimal" reference values [23] was meaningless. However, a few facts of general interest could be pointed out. EDT showed markedly shorter values any time source and receivers were in the same sub-space and this sub-space was not the main nave. This may certainly be considered an effect of the reduced source-receiver distance, but the same effect appeared at distances beyond the reverberant radius, thus being related to the sub-space properties. Variations were about 2 s, equivalent to subjective difference varying between 7 and 11 JNDs, depending on the church, thus being clearly audible and allowing improved acoustic conditions.

Another result worth being mentioned was the increased clarity observed in SPB when source was in A. In fact, while in most of the other churches C_{80} was below –5 dB beyond approximately 20 m, in SPB C_{80} remained above that limit up to 60 m. However, in the same receivers G was as low as –5 dB, suggesting that listeners perceive a clear but relatively weak sound. Conversely, in SJL most of the receivers in the nave have positive G values, and up to about 30 m from the source they also have C_{80} greater than –5dB, suggesting a generally improved listening experience which, as in SPB was supported by direct sound and early reflections from the larger pillars. In support of this, all the receivers not getting direct sound and located in secondary sub-volumes showed dramatically lower C_{80} values (with differences as big as 15 dB in some cases) and G values (with differences of about 3 dB). This was evident in both the cases in which the organ position was considered. In particular, in SPX the organ position is in the transept and both nave and isles only receive indirect sound, resulting in a marked shift in all the measured values.

In terms of spaciousness SMM showed the best behaviour, with an average 1–IACC value of 0.70 nearly independent of source position. Narrower proportions and presence of columns contributed to this result. The semi-outdoor conditions observed in SPB resulted in generally lower values, with an average of 0.4 that increased to 0.48 when source was the organ, In SJL and SPX 1–IACC values were higher and comparable to SMM when the source moved in the choir/organ, while at the altar they dropped by about 0.10 as a consequence of stronger direct sound and weaker lateral reflections.

4.2. Effect of coupled volumes

In order to better explain some of the above results and put them in a broader context, a more detailed discussion was needed. The first important topic requiring attention referred to what in some of the oldest papers [28,29] was recognized as an unusually shorter reverberation time, compared to actual room volumes. In order to explain such unusual behavior, weak coupling between different sub-volumes was hypothesized to remove acoustic energy from the main volumes[29] and they also calculated a "fictitious" absorption coefficients for the openings. Raes and Sacerdote [28] pointed out the great difference between the acoustics in SJL and SPX, with the first having shorter reverberation time despite the relatively similar volume, with significant differences between nave and aisles. Difference in ornamentation was suggested as a possible explanation. The same topic was already addressed with reference to BSP[17], showing that coupling between sub-volumes was not responsible for the lower reverberation in that church. In fact, reverberation time of the coupled-volume system was actually longer than the value resulting from application of classical formulas assuming exactly the same absorption distribution. So, it was concluded that increased sound absorption from richly decorated surfaces, as demonstrated by means of scale model measurements, was the most convincing explanation.

The same procedure previously applied to BSP was consequently applied to the other three churches in order to better understand the observed behavior with particular reference to energy-based parameters. Geometrical acoustic analysis was first carried out using simplified 3D geometrical models of the churches as input and by properly calibrating sound absorption coefficients. The same models, were also employed to derive the geometrical data required to carry out the statistical acoustic (SA) analysis consisting in the solution of a system of energy balance equations [31] applied to the sub-volumes into which each church was divided. For the sake of brevity only results of SA analysis at the 1 kHz octave band were presented here.

Even though some improvements have been proposed to take into account actual source-receiver distance [8,37]. Summers [37] also demonstrated that such modifications offer little advantage in terms of accuracy compared to the increased computational burden. Thus, the classical approach was applied here. The main advantage of this approach being its fully parametric solution and, consequently, the possibility to easily compare different conditions in a short time, with no dependence on random processes. A possible disadvantage is that under certain conditions (such as strong coupling), results may not be as reliable as expected. However, availability of measured results easily allows to detect such condition. Among the different criteria proposed to quantify acoustic coupling between sub-volumes [31], the coupling factor defined by Cremer and Muller[38] was preferred:

$$k_i = \frac{S_i}{A_i + S_i} \ , \qquad (1)$$

where A_i is the total sound absorption (including air) and S_i is the sum of the opening areas inside each sub-volume. It yields strong coupling when $k_i \approx 1$ and weak coupling when $k_i \approx 0$.

Assigning absorption coefficients (α) to the different surfaces was one of the most delicate issues in order to have significant results. Materials with no big difference among the surveyed churches were given the same α, possibly deriving them from consolidated literature [17,18,39]. Surfaces that are specific of a church were given absorption coefficients derived from iterative adjustment aimed at matching measured and simulated acoustic parameters among the different octave bands in the geometrical acoustic models (Table 2). As visual inspection of wooden ceiling showed little differences among churches (Fig. 2), it was given the same α, with the exception of the side aisles in SPX that, having larger lacunars and less rich decorative patterns, were given lower values at medium-high frequencies. In SJL the richly decorated plaster surfaces of the main nave were given the same α of SPB. Finally, in SMM the niches in the side aisles were assigned higher α because they had sculptures and included wooden confessionals in each bay.

Table 2
Summary of the absorption and scattering coefficients used in the GA and SA models

	Absorption coefficients					
	125	*250*	*500*	*1k*	*2k*	*4k*
Marble floor [39]	0.01	0.01	0.2	0.02	0.03	0.03
Glass [39]	0.30	0.20	0.14	0.10	0.05	0.05
Pews [18, Model F]	0.05	0.10	0.18	0.21	0.21	0.21
Plastic seats[39]	0.06	0.10	0.10	0.20	0.30	0.20
Coffered vaults (plastered) [17]	0.20	0.20	0.20	0.25	0.25	0.25
Coffered ceiling	0.45	0.40	0.35	0.35	0.35	0.35
Wooden ceiling [*SPX]	0.37	0.25	0.20	0.20	0.20	0.20
Scarcely decorated walls [39]	0.02	0.02	0.03	0.03	0.05	0.05
Decorated hard surf. [17]	0.04	0.04	0.06	0.07	0.08	0.08
Niches w/ wooden parts[*SMM]	0.17	0.20	0.18	0.18	0.18	0.18
Columns/Pillars[17]	0.04	0.04	0.05	0.05	0.06	0.06
Sculptures[17]	0.12	0.12	0.15	0.15	0.18	0.18

*Values obtained from iterative adjustment for each specific church

Then, each church was sub-divided into 19 sub-volumes aimed at obtaining the lowest coupling factor, while preserving subspace specificity (Fig. 10). Naves and aisles were divided into sub-volumes (following the same proposal by Chu and Mak[8]), even though the coupling area between adjacent spaces was clearly high. As shown in Fig. 11, coupling factors were higher in SPX and SMM, with most of the values varying between 0.78 and 0.86, while lower values were observed in SJL (between 0.72 and 0.83), and even smaller in SPB (between 0.55 and 0.63). The thin columns dividing naves and aisles in the first two churches clearly explained the stronger coupling, while the smaller apertures (compared to nave dimension) in SPB explained its weaker coupling. The maximum values, generally observed in the crossing, were similar in all the cases and rarely exceeded 0.9.

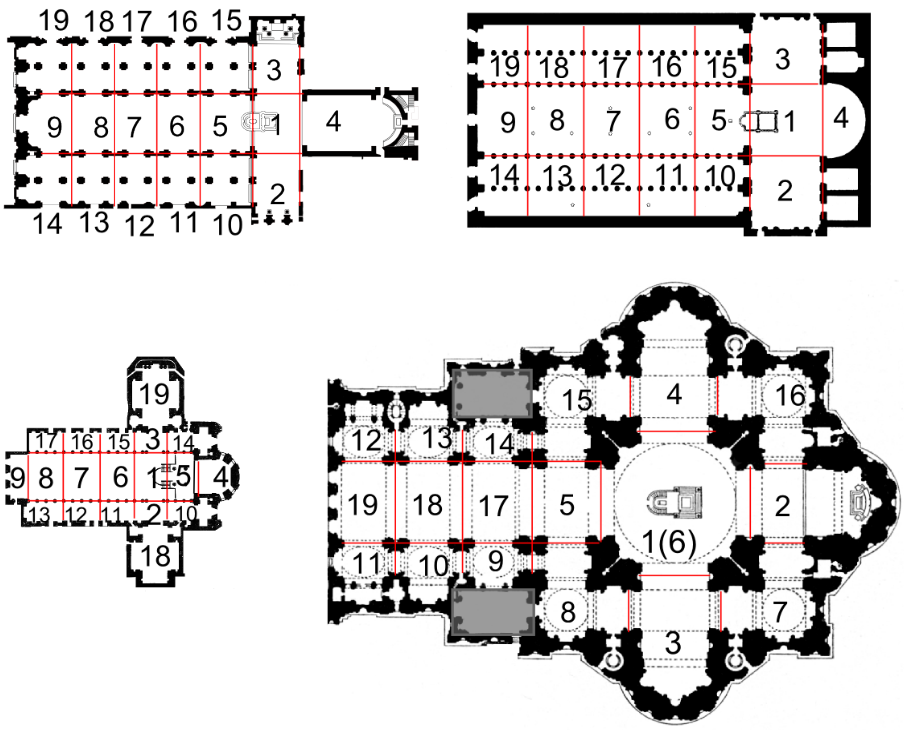

Figure 10 – Schematic view of the subdivision of the four basilicas into sub-volumes used in SA model. Each sub-volume is identified by a different number. Value in brackets (in SPB) correspond to the dome.

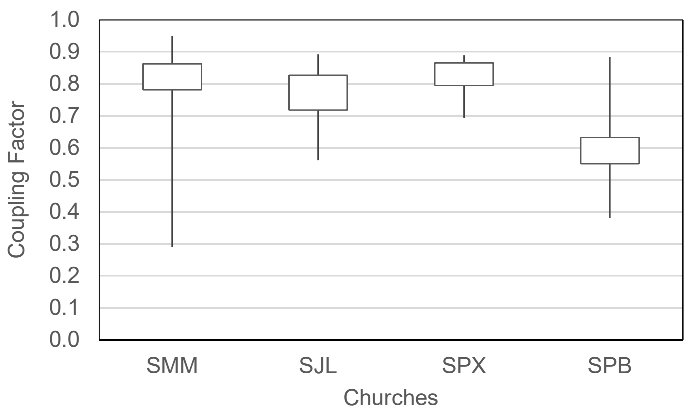

Figure 11 – Box plot of the coupling factors calculated in the four basilicas. Boxes correspond to the 1st and 3rd quartile, while error bars correspond to minima and maxima.

The last action required was that of assigning the fraction of direct sound pertaining to each sub-space[31] which was calculated by numerical integration as the fraction of the total solid angle subtended by the coupling surface as viewed from the source. Correct estimation of this value, taking into account actual acoustic behavior of possible obstacles, proved to be of major importance to achieve correct estimation of all the energy-based parameters. Eyring's absorption exponents were used in calculations, recalling that in SPB they returned more accurate results at medium-high frequencies[17].

Accuracy of results was assessed in terms of just noticeable difference (JND)[33,40]. Results proved significantly accurate (Fig 12), even in predicting the discrepancies found in SPX when source F was used. Differences were generally below 2 JNDs between predicted values and the average of those measured in the same sub-volume (Table 3). The only exceptions were usually found in sub-spaces where strong reflections were likely to increase the initial fraction of direct energy, or where transmission through adjacent sub-volumes allowed more direct sound to enter (typically the farthest sub-spaces). Thus, despite the higher coupling factors, application of SA model proved effective in all the four basilicas, allowing a straightforward explanation of most of the anomalies observed when plotting values as a function of distance, as a consequence of the different energy distribution in each sub-volume.

Table 3

Summary of average absolute JND differences calculated between measured and values predicted using SA model of coupled volumes at 1 kHz.

	SMM	*SJL*	*SPX*	*SPX (F)*	*SPB*
T30	0.6	0.7	0.8	0.9	0.3
EDT	1.1	1.5	1.0	1.9	0.9
G	1.2	0.9	1.1	1.4	1.3
Ts	0.9	1.6	1.6	0.7	1.8

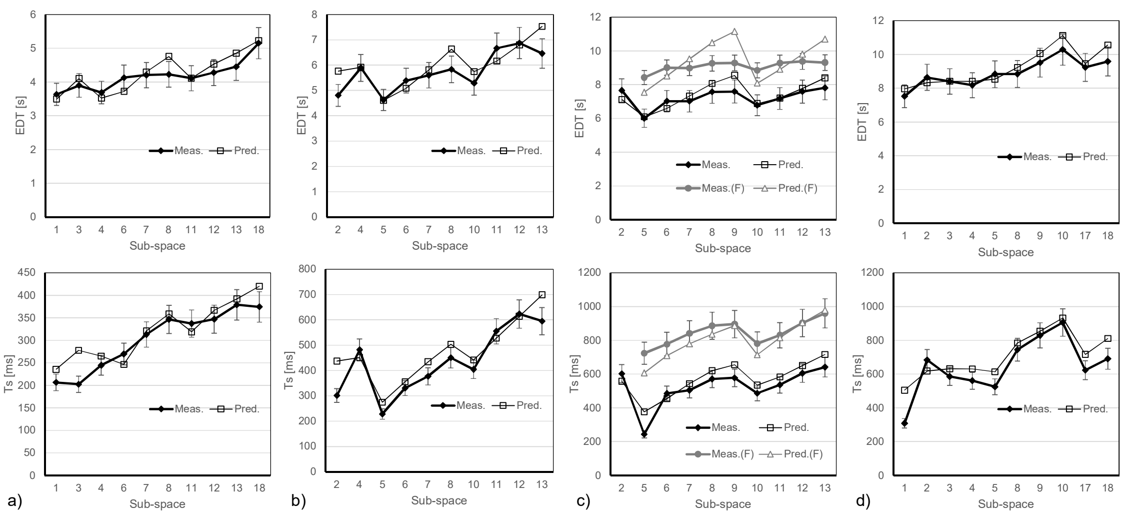

Figure 12 – Plot of average of measured values at 1 kHz octave band, inside each sub-volume and the corresponding values predicted using SA model of coupled volumes. a) SMM; b) SJL; c) SPX; d) SPB. Error bars correspond to JND.

The percent difference between the reverberation time of the coupled volume system (T_{CV}, assumed as the longest decay term resulting from the analytical solution) and that calculated using classical formulas referred to the whole volume (T_{Eyr}), and subsequently indicated as $\Delta T_{\%cv}$ offered interesting elements of discussion. As anticipated, in SPB $\Delta T_{\%cv}$ was about 12%, while it was much smaller in the other churches (Table 4). Explanation for such a large difference could be tentatively found in the different coupling factors observed in the churches. So, the weaker coupling in SPB caused the absorption distributed inside "secondary" volumes to be less effective than it would have been if applied to a single volume.

Table 4
Summary of the percent differences ($\Delta T_{\%cv}$) between reverberation time calculated according to classical formulas (T_{Eyr}) and that calculated using coupled-volumes system (T_{cv}) in the four surveyed churches. Ki is the median coupling factor.

	Ref			α=0.05				α=0.10				α=0.15			
	T_{eyr}	T_{cv}	$\Delta T_{\%cv}$	T_{eyr}	T_{cv}	$\Delta T_{\%cv}$	Ki	T_{eyr}	T_{cv}	$\Delta T_{\%cv}$	Ki	T_{eyr}	T_{cv}	$\Delta T_{\%cv}$	Ki
SMM	4.11	4.13	0.5%	8.08	8.18	1.2%	0.88	4.52	4.65	2.9%	0.80	3.08	3.22	4.5%	0.73
SJL	5.73	5.74	0.2%	9.24	9.66	4.5%	0.83	5.15	5.61	8.9%	0.72	3.51	3.95	12.5%	0.63
SPX	7.09	7.11	0.3%	11.07	11.37	2.7%	0.88	6.52	6.93	6.3%	0.81	4.54	4.97	9.5%	0.74
SPB	8.00	8.88	11.0%	12.89	13.33	3.4%	0.76	7.74	8.34	7.8%	0.66	5.44	6.09	11.9%	0.58

However, in order to better clarify the nature of this variation, a final test was made by assigning exactly the same absorption coefficients (conventionally assumed equal to 0.05, 0.10, and 0.15) to all the room surfaces of each church. Under such conditions, $\Delta T_{\%cv}$ changed significantly, with differences more evenly distributed and showing an apparently linear dependence on the absorption coefficient (Table 4). In particular, churches with the lowest coupling factors showed higher $\Delta T_{\%cv}$ and vice versa. By increasing α the coupling factor decreased, and, consequently, $\Delta T_{\%cv}$ grew. However, under uniformly distributed absorption $\Delta T_{\%cv}$ was always larger than the values initially observed in SMM, SJL, and SPX, (e.g. in SJL the variation was larger than in SPB). This suggested that position of sound absorbing materials was equally important as in those churches a large fraction of total absorption was located in the main volumes (nave, choir/apse, and transepts). The above results provided evidence that trying to explain the reduced reverberation time only as a consequence of acoustic coupling among volumes (as suggested in Ref. 29) was incorrect. In fact, the opposite is true as the presence of coupled volumes increased reverberation time. Anyway, concentrating sound absorption in the largest (and strongly coupled) volumes reduced such differences and made the space behave more like a single volume.

DOI: 10.1016/j.jsv.2016.07.007

5. Conclusions

The analysis of the IRs measured in the four Papal basilicas in Rome offered interesting elements of discussion. T_{30} showed variations that were explained as a function of different dimensions and surface finishing. In particular, large decorative patterns both on walls and on coffered ceilings realistically determined an increase in absorption coefficients. Significant variations in EDT were found inside each church. In particular, when source and receivers were in the same sub-space shorter EDT values appeared and decays showed the clear presence of two slopes. This was explained as a consequence of acoustic coupling between the different volumes of each church. The effects shown in Fig. 4 were found also when SA model was applied under the same conditions. Energy-based parameters, such as G, and C_{80} normally follow a decreasing trend in churches. However, in this case several anomalies were observed. Acoustic coupling once again explained most of the differences found between nave and aisles, while the differences found in C_{80} measured in different churches at nearly the same distances were explained as a consequence of the different energy density pertaining to each church. Thus, even though in SPB T_{30} was longer than in other churches, C_{80} remained high, at least as far as the direct sound could get to receivers. Among spaciousness parameters, a narrow plan combined with the presence of columns increased 1–IACC in SMM. In other churches with columns (SPX and SJL) only receivers located behind them showed increased 1–IACC values. SPB showed markedly reduced values, likely as a consequence of the stronger direct sound compared to diffuse reflections. Finally, application of the SA model proved effective despite the different, and sometimes high, coupling levels, showing that under uniform absorption distribution a lower coupling factor caused significant discrepancies with T_{30} predicted using classical formulas. Conversely, when most of the absorption was in the largest volumes, the differences between coupled-volume reverberation and classical formulas tended to fade.

In conclusion, the acoustical analysis of the four Papal basilicas in Rome offered the opportunity to better understand how sound propagates in large and complex spaces, where coupling effects may play a major role to explain how acoustic energy distributes among sub-spaces, also depending on source and receivers positions. Even though further investigations are needed to better investigate how these features were matched with different usage that, along time, has been made of different spaces (chapels, choirs), from the analytical point of view the application of the coupled-volume model proved extremely promising in such complex spaces.

References

[1] A.P.O. Carvalho, Relations between rapid speech transmission index (RASTI) and other acoustical and architectural measures in churches. Applied Acoustics, Vol 58, 1999, 33-49.

[2] M. Mijic, Serbian Orthodox Church – an acoustical view. Proc. 17th ICA, Rome, Italy, 2-7 September 2001.

[3] M. Galindo, T. Zamarreño, S. Girón, Acoustic analysis in Mudejar-Gothic churches: Experimental results, J. Acoust. Soc. Am. 117 (2005) 2873-2888.

[4] Z. Engel, K. Kosala, Acoustic properties of selected churches in Poland. Mechanics Vol 24 (3), (2005) 173-181.

[5] E. Cirillo, F. Martellotta, Worship, acoustics, and architecture. Multi-science publishing, Brentwood, 2006.

[6] V. Desarnaulds, A.P.O. Carvalho, G. Monay, Church Acoustics and the Influence of Occupancy, Build. Acoust. 9 (2009) 29–47.

[7] F. Martellotta, E. Cirillo, A. Carbonari, P. Ricciardi, Guidelines for acoustical measurements in churches, Appl. Acoust. 70 (2009) 378–388.

[8] Y. Chu, C.M. Mak, Early energy decays in two churches in Hong Kong, Appl. Acoust. 70 (2009) 579–587.

[9] C.R. Jiménez-Dianderas, Acoustical behaviour of colonial churches in Cusco, Peru, in: 161 Meet. Acoust. Soc. Am. Seattle, 23-27 May 2011, 2011.

[10] T. Zakinthinos, D. Skarlatos, The effect of ceramic vases on the acoustics of old Greek orthodox churches, Appl. Acoust. 68 (2007) 1307–1322.

[11] Y. Soeta, K. Ito, R. Shimokura, S.-I. Sato, T. Ohsawa, Y. Ando, Effects of sound source location and direction on acoustic parameters in Japanese churches, J. Acoust. Soc. Am. 131 (2012) 1206–1220.

[12] J.C. Valière, B. Palazzo-Bertholon, J.D. Polack, P. Carvalho, Acoustic pots in ancient and medieval buildings: Literary analysis of ancient texts and comparison with recent observations in French churches, Acta Acust. United with Acust. 99 (2013) 70–81.

[13] L. Álvarez-Morales, T. Zamarreño, S. Girón, M. Galindo, A methodology for the study of the acoustic environment of Catholic cathedrals: Application to the Cathedral of Malaga, Build. Environ. 72 (2014) 102–115.

[14] P. Brezina, Measurement of intelligibility and clarity of the speech in Romanesque churches, J. Cult. Herit. 16 (2015) 386–390.

[15] T. Zamarreño, S. Girón, M. Galindo, Acoustic energy relations in Mudejar-Gothic churches., J. Acoust. Soc. Am. 121 (2007) 234–250.

[16] F. Martellotta, A multi-rate decay model to predict energy-based acoustic parameters in churches (L), J. Acoust. Soc. Am. 125 (2009) 1281–1284.

[17] F. Martellotta, Identifying acoustical coupling by measurements and prediction-models for St. Peter's Basilica in Rome., J. Acoust. Soc. Am. 126 (2009) 1175–1186.

[18] F. Martellotta, E. Cirillo, Experimental studies of sound absorption by church pews, Appl. Acoust. 70 (2009) 441–449.

[19] L. Alvarez-Morales, F. Martellotta, A geometrical acoustic simulation of the effect of occupancy and source position in historical churches, Appl. Acoust. 91 (2015) 47–58.

[20] R. Suárez, J.J. Sendra, A. Alonso, Acoustics, Liturgy and Architecture in the Early Christian Church. From the domus ecclesiae to the basilica, Acta Acust. United with Acust. 99 (2013) 292–301.

[21] A. Pedrero, R. Ruiz, A. Díaz-chyla, C. Díaz, Acoustical study of Toledo Cathedral according to its liturgical uses, Appl. Acoust. 85 (2014) 23–33.

[22] K. Kosała, Z.W. Engel, Assessing the acoustic properties of Roman Catholic churches: A new approach, Appl. Acoust. 74 (2013) 1144–1152.

[23] F. Martellotta, Subjective study of preferred listening conditions in Italian Catholic churches, J. Sound Vib. 317 (2008) 378–399.

[24] J. Segura, A. Barba, A. Planells, S. Cerdá, A. Giménez, R.M. Cibrián, Acoustical reconstruction of a church in ruins: The monastery of Santa Maria de la Murta. Proceedings of the Forum Acusticum 2014, Kraków, Poland 7-12 September 2014.

[25] A. Pedrero, A. Díaz-Chyla, C. Díaz, S. Pelzer, M. Vorländer, Virtual restoration of the sound of the Hispanic Rite, in: Proc.. Forum Acust., 2014.

[26] J. Meyer, Kirchenakustik. Verlag Erwin Bochinsky, Frankfurt am Main, 2003.

[27] M. Kleiner, D. Klepper, R. Torres, Worship space acoustics, J. Ross Publishing, 2010.

[28] A.C. Raes, G.G. Sacerdote, Measurements of the Acoustical Properties of Two Roman Basilicas, J. Acoust. Soc. Am. 25 (1953) 954–961.

[29] R.S. Shankland, H.K. Shankland, Acoustics of St. Peter's and Patriarchal Basilicas in Rome, J. Acoust. Soc. Am. 50(2) (1971) 389–396.

[30] N. Xiang, P. Goggans, T. Jasa, P. Robinson, Bayesian characterization of multiple-slope sound energy decays in coupled-volume systems, J. Acoust. Soc. Am. 129 (2011) 741–752.

[31] J.E. Summers, R.R. Torres, Y. Shimizu, Statistical-acoustics models of energy decay in systems of coupled rooms and their relation to geometrical acoustics, J. Acoust. Soc. Am. 116 (2004) 958–969.

[32] J.S. Anderson, M. Bratos-Anderson, Acoustic Coupling Effects in St Paul's Cathedral , London, J. Sound Vib. 236 (2000) 209–225.

[33] ISO 3382-1, Acoustics – Measurement of room acoustic parameters -- Part 1: Performance spaces. ISO, Geneva, Switzerland, (2009)

[34] S. Müller, P. Massarani, Transfer-function measurement with sweeps, J. Audio Eng. Soc. 49, (2001) 443–471.

[35] S. Girón, M. Galindo, T. Zamarreño, Distribution of lateral acoustic energy in Mudejar-Gothic churches, J. Sound Vib. 315 (2008) 1125–1142.

[36] H. Sakai, S. Sato, Y. Ando, Orthogonal acoustical factors of sound fields in a forest compared with those in a concert hall, J. Acoust. Soc. Am. 104 (1998) 1491–1497.

[37] J.E. Summers, Accounting for delay of energy transfer between coupled rooms in statistical-acoustics models of reverberant-energy decay, J. Acoust. Soc. Am. 132 (2012) EL129–EL134.

[38] L. Cremer, H.A. Muller, Principles and Applications of Room Acoustics, volume 1. Applied Science, London, 1982.

[39] M. Vorländer, Auralization, fundamentals of acoustics, modelling, simulation, algorithms and acoustic virtual reality. Springer-Verlag, Berlin, 2008.

[40] F. Martellotta, The just noticeable difference of center time and clarity index in large reverberant spaces, J. Acoust. Soc. Am., 128(2), (2010), 654-663